ARTICLE
Journal of Cellular Biochemistry 116:1278–1285 (2015)

Journal of Cellular Biochemistry

# Computational Simulation Techniques to Understand Rifampicin Resistance Mutation (S425L) of *rpoB* in *M. leprae*

Nisha J. and Shanthi V.*

*Industrial Biotechnology Division, School of Bio Sciences and Technology, VIT University, Vellore 632014, Tamil Nadu, India*

## ABSTRACT

*Mycobacterium leprae*, the etiologic agent of leprosy, is non-cultivable in vitro. Consequently, the assessment of antibiotic activity against *M. leprae* hinge mainly upon the time consuming mouse footpad system. As *M. leprae* develops resistance against most of the drugs, the evolution of new long acting antimycobacterial compounds stand in need for leprosy control. The *rpoB* of *M. leprae* is the target of antimycobacterial drug, rifampicin. Recently, cases were reported that *rpoB* mutation (S425L) became resistant to rifampicin and the mechanism of resistance is still not well understood. The present study is aimed at studying the molecular and structural mechanism of the rifampicin binding to both native and mutant *rpoB* through computational approaches. From molecular docking, we demonstrated the stable binding of rifampicin through two hydrogen bonding with His420 residue of native than with mutant *rpoB* where one hydrogen bonding was found with Ser406. The difference in binding energies observed in the docking study evidently signifies that rifampicin is less effective in the treatment of patients with S425L variant. Moreover, the molecular dynamics studies also highlight the stable binding of rifampicin with native than mutant (S425L) *rpoB*. J. Cell. Biochem. 116: 1278–1285, 2015. 

**KEY WORDS:** *rpo*B; RIFAMPICIN; DRUG RESISTANCE; HOMOLOGY MODELING; MOLECULAR DYNAMICS SIMULATIONS

Leprosy is a chronic infectious disease caused by an obligate intracellular pathogen *M. leprae*. As no vaccine at hand, early diagnosis, and treatment is the primary strategy to control leprosy. Treatment mainly relies on Multidrug therapy (MDT), recommended by World Health Organization (WHO) [WHO, 1982, 1998]. As reported by WHO, MDT conceived for leprosy has been significant at reducing both its prevalence and incidence globally [Jamet et al., 1995]. As stated by the official figures from 115 countries, at the end of 2012, the global registered prevalence of leprosy was 189,018 and the reported new cases were 232,857 [WHO, 2010].

The MDT regimens for leprosy contain rifampicin (RMP), (3-{[(4-methyl-1-piperazinyl)-imino]-methyl}rifamycin) [Williams et al., 2012]. The bactericidal effect of RMP is operative greater than any combination of the other drugs and hence, RMP is the backbone of the MDT regimens [Ji et al., 1996, 1998]. A single dose of 1,200 mg can lessen the viable bacilli in a patient's skin to undetectable levels within a few days [Matsuoka, 2010]. Disclosure of RMP resistance turns out very great issues for treating individual patients; its global dissemination is alarming to reach the leprosy elimination target [WHO, 1999]. RMP resistant leprosy was proved as early as the 1970s [Jacobson et al., 1976]. The major restraints in testing drug-susceptibility by the mouse foot pad technique are time and expense. Another constraint reported is that, to preserve the viability of the *M. leprae* contained in biopsy specimens and to prevent growth of contaminants [Ji, 1987].

The β subunit of DNA-dependent RNA polymerase, encoded by *rpoB* gene is the target of RMP. RMP binding to the β subunit inhibits DNA-dependent mRNA transcription [Musser, 1995]. *M. tuberculosis* resistance to RMP harmonize with the structural changes of the β-subunit of the RNA polymerase, primarily due to missense mutations that occur within a highly conserved region of the *rpoB* gene mentioned to the RMP resistance determining region [Telenti et al., 1993; Honore et al., 1993]. RMP resistance in *M. leprae* also agrees with missense mutations within the *rpoB*. Substitutions within codon Ser425 exhibited to be the most frequent mutations associated with the development of the RMP-resistant phenotype in *M. leprae* [Williams et al., 1994; Ji, 2002; Williams et al., 2012].

Relapse and emergence of drug resistance are customary in antimicrobial therapy, and there is no rationale to be convinced that

Grant sponsor: ICMR; Grant number: 5/8/3/5/TF.Lep/2012-ECD-I.
*Correspondence to: Dr. V. Shanthi, Industrial Biotechnology Division, School of Bio Sciences and Technology, VIT University, Vellore 632014, Tamil Nadu, India. E-mail: shanthi.v@vit.ac.in
Manuscript Received: 9 October 2014; Manuscript Accepted: 16 January 2015
Accepted manuscript online in Wiley Online Library (wileyonlinelibrary.com): 10 February 2015
DOI 10.1002/jcb.25083 • © 2015 Wiley Periodicals, Inc.

the MDT for treatment of leprosy would be an exception. Because RMP is the unique component of the MDT regimens for leprosy, and as >10 million leprosy patients have completed their treatment with MDT, the magnitude of the emergence of RMP resistance should be under surveillance [WHO, 1999].

Much remains to be learned about the molecular genetic basis of RMP resistance in *M. leprae*. In reality, the identification of the RMP interactions with native and mutant *rpoB* using crystallography has been very laborious. Thus, we need to rely on molecular modeling and docking studies to gain further insights into these interactions. However, the structural detail of the RMP–*rpoB* interaction is left unknown. In addition, the molecular basis for the binding specificities and affinities are still undetermined. Therefore, in the present investigation, molecular simulation studies were initiated not only to understand the binding mechanism but also to simulate the potential conformational movements of both the native and mutant *rpoB* with the ligand to impart notable insights into structure–function relationships.

## METHODOLOGY

### HOMOLOGY MODELING

The sequence of *M. leprae rpoB* was retrieved from the UniprotKB database, http://www.uniprot.org (Accession no: P30760) and used for modeling the *rpoB* of *M. leprae*. Homology modeling of native *rpoB* was executed by SWISS-MODEL [Schwede et al., 2003] and the modeled native *rpoB* was mutated computationally at position 425 as S425L using Swiss-Pdb viewer [Guex et al., 1997]. Both the native and mutant *rpoB* models were visualized and subjected to energy minimization using Merck Molecular Force Field 94 (MMFF94) implemented in YASARA software package [Halgren, 1996; Krieger et al., 2002]. Further, the optimized model was put through quality assessment with respect to its geometry and energy aspects. Finally, the native and mutant *rpoB* models were validated by inspection of the $\Phi/\Psi$ angle using Ramachandran plot [Ramachandran et al., 1963] obtained from PROCHECK analysis [Laskowaski et al., 1993].

### LIGAND OPTIMIZATION

RMP (CID 5381226), the ligand was downloaded from the Pubchem database (http://pubchem.ncbi.nlm.nih.gov.in), in Standard Delay Format (SDF). Conversion of SDF format into Protein Data Bank (PDB) format was made using Open Babel program [Boyle et al., 2011]. The MMFF94 force field [Halgren, 1996] implemented in YASARA package [Krieger et al., 2002] was employed for energy minimization of RMP structure. Following which the ligand atoms were added with Gasteiger partial charges, non-polar hydrogen atoms were integrated and rotatable bonds were defined. Moreover, the ligand geometries and electric properties were computed using Molecular Orbital PACkage 2009 [Stewart, 1990].

### DOCKING STUDIES

With a view to explore the active site of *rpoB* of *M. leprae* and its ligand specificity, the protein–ligand interaction analysis was executed.

AutoDockVINA [Trott et al., 2010] embedded into the YASARA Structure package [Krieger et al., 2002], was applied to dock RMP to the refined protein models of native and mutant *rpoB* by running 25 of Global Docking. In YASARA, the docking runs of the ligand to protein generated results, graded by binding energy where more positive energies implies stronger binding, and negative energies corresponds to no binding. Most of the docking program available in the literature results binding energy in negative values. However, in the present investigation docking analysis was performed by means of YASARA algorithm. In YASARA, docking runs of the ligand to receptor yield results sorted by binding energy where more positive energies indicate stronger binding and negative energies equate to less or no binding. This is mainly because of the difference in the YASARA binding energy function. The energy is calculated as the difference between the sum of potential and solvation energies of the separated compounds and the sum of potential and solvation energies of the complex in the YAMBER3 force field. Thus, more positive energy (difference) indicates the higher affinity between drug and target structure [Jakubik et al., 2013]. The best 10 clusters according to the AutoDockVINA score were generated for both the *rpoB* models. The top ranked confirmation of native and mutant *rpoB* complex was selected for further analysis.

Subsequently, we employed LIGPLOT program [Wallace et al., 1995] to investigate the hydrogen bond interactions existing in *rpoB* of native and mutant complexes.

### MOLECULAR DYNAMICS (MD) SIMULATIONS

The docked complexes viz., native *rpoB*-RMP complex and mutant *rpoB*-RMP complex were treated with MD simulations to delineate diverse structural traits. All simulations were achieved through GROMACS package 4.6.3 [Spoel et al., 2005] applying GROMOS43a1 force field [Gunsteren et al., 1996]. The structures were solvated in Simple point charge (SPC) water model [Meagher et al., 2005] in a 0.9 nm cubic box with periodic boundary conditions. The ligand topology was generated with the aid of PRODRG server [Schuttelkopf et al., 2004]. The protein–ligand complex was minimized for 1,000 steepest descent steps. After energy minimization, the system was equilibrated at constant temperature and pressure. The equilibrated structures were then put through molecular dynamic simulations for 15,000 ps, and the integration time step was set to 2 fs. The non-bonded list was made, using an atom-based cutoff of 8 Å. The long range electrostatic interactions were computed with a 1.0 nm cutoff by the particle-mesh Ewald algorithm [Darden et al., 1999]. Total of 0.9 nm cutoff was enlisted to Lennard–Jones interaction for computing non bonded interactions. Subsequently, LINCs algorithm [Lindahl et al., 2001] was employed for constraining bond lengths engaging hydrogen atoms. Finally, the systems were treated with 15 ns MD simulations enabling the movements of all atoms and the trajectory snapshots were extracted at every picosecond for structural analysis. Root Mean Square Deviation (RMSD), Root Mean Square Fluctuations (RMSF), and Solvent Accessible Surface Area (SASA) were measured through Gromacs utilities g_rms, g_rmsf, and g_sasa, respectively.

## RESULTS & DISCUSSION

### MODEL BUILDING AND VALIDATION

The native *rpoB* model of *M. leprae* was built with the sequence of *M. leprae rpoB* acquired from the UniprotKB database (Accession no:

P30760) with SWISS-MODEL [Schwede et al., 2003] and a mutated *rpoB* model was also created by Swiss Pdb viewer [Guex et al., 1997] with the aid of modeled native *rpoB* as template (Fig. 1a and b). The predicted model quality was evaluated by PROCHECK [Laskowaski et al., 1993] which unveiled that 83.6% residues of native *rpoB* were found in most favored regions and 16.4% of residues in additionally allowed regions (Fig. 2). Comparably, 83.6% residues of mutant *rpoB* were found in most favored regions and 16.4% of residues in additionally allowed regions. Hence the total 100% of residues of both native and mutant *rpoB* models were found in the favored regions strongly suggesting the good quality of the model.

## MOLECULAR DOCKING STUDIES

In the present docking study, the binding affinity and the interactions found between RMP and both the native and mutant *rpoB* of *M. leprae* were assessed using binding energy and contacting residues. From the Table I, the binding energy of native *rpoB*–RMP complex was found to be 7.324 kcal/mol and that of mutant *rpoB*–RMP complex was found to be 6.865 kcal/mol. The binding energy for mutant *rpoB*–RMP complex was found lesser than the native *rpoB*–RMP complex. This clearly indicated that mutation at position S425L in the *rpoB* structure found to affect the binding of RMP. Besides, the RMP contacting residues of native *rpoB* was found to be Phe at position 399, Phe at 400, Leu at 405, Ser at 406, Gln at 407, Met at 409, His at 420, Lys at 421, Arg at 423, Leu at 424, Ser at 425, and Pro at 429 and that of mutant *rpob* was found to be Phe at 399, Phe at 400, Gly at 401, Leu at 405, Ser at 406, Gln at 407, Phe at 408, Met at 409, His at 420, Lys at 421, Arg at 423, Leu at 424, and Leu at 425. The docked complexes were shown in Figure. 3a and b.

In order to investigate the effect of mutation S425L on the binding of RMP, we examined the intermolecular interactions in the native and mutant *rpoB*–RMP complex. The LIGPLOT tool was used to investigate the intermolecular interactions and the results were shown in Figure 4a and b. The results from our analysis clearly indicate that parameters such as number of hydrogen bonds and the binding residues are certainly important for the understanding structural and functional impact of *rpoB* S425L mutation. It is clear from the Figure 4 that two intermolecular contacts exist in the native type complex structures whereas only one interaction was observed in the mutant type. This prime difference is mainly because of the difference in the binding pocket residues. For instance, His 420 unveiled two hydrogen bonds whereas Ser406 unveiled only one hydrogen bond interaction with RMP in the native- and mutant-type complexes, respectively. This highlights that S425L mutation significantly alter the conformations of the binding pocket residues in the *rpoB* structure [Rajasekaran et al., 2011]. This results in the improper binding of RMP with the target protein and thus confers drug resistance. Consequently, we further continued the investigation on the effects of mutation by MD simulation to gain greater understanding into the stability of these complexes.

## MOLECULAR DYNAMICS SIMULATION

MD simulation was carried out by GROMACS 4.6.3 [Spoel et al., 2005] which aimed to simulate the structural stability and dynamical changes of both native and mutant type *rpoB*–RMP complexes. The geometrical and conformational properties such as RMSD, RMSF, and SASA were examined from the MD trajectories. The RMSD analysis over the simulation time is certainly helpful for the

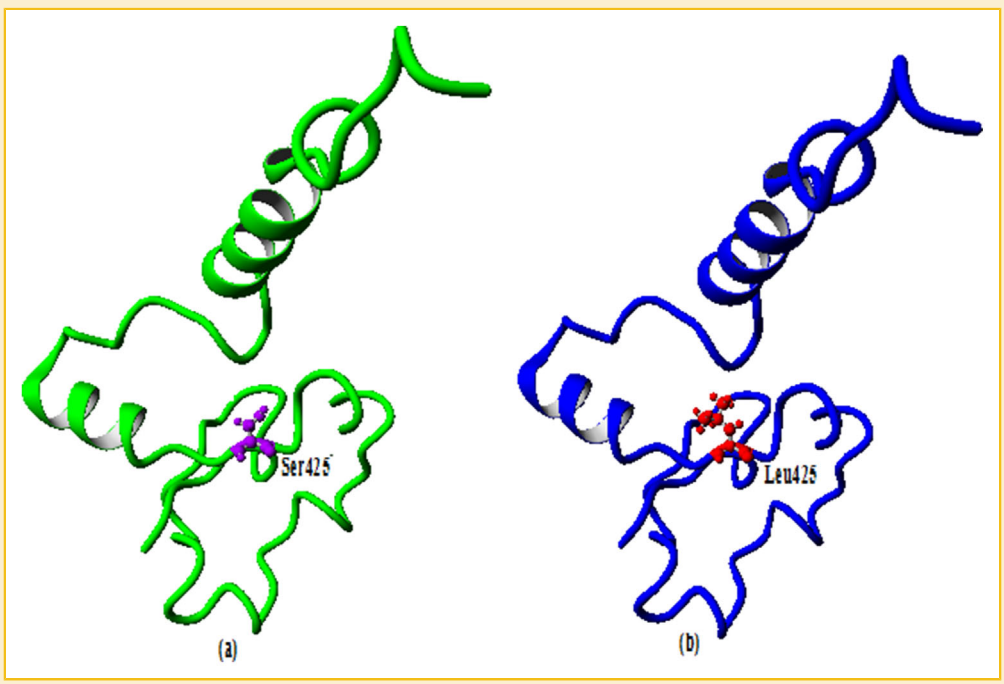


**Fig. 1.** Homology modeling of the structure of *M. leprae rpoB*. Modeled structure of native *rpoB* (A). Mutant (S425L) structure of *rpoB* (B).

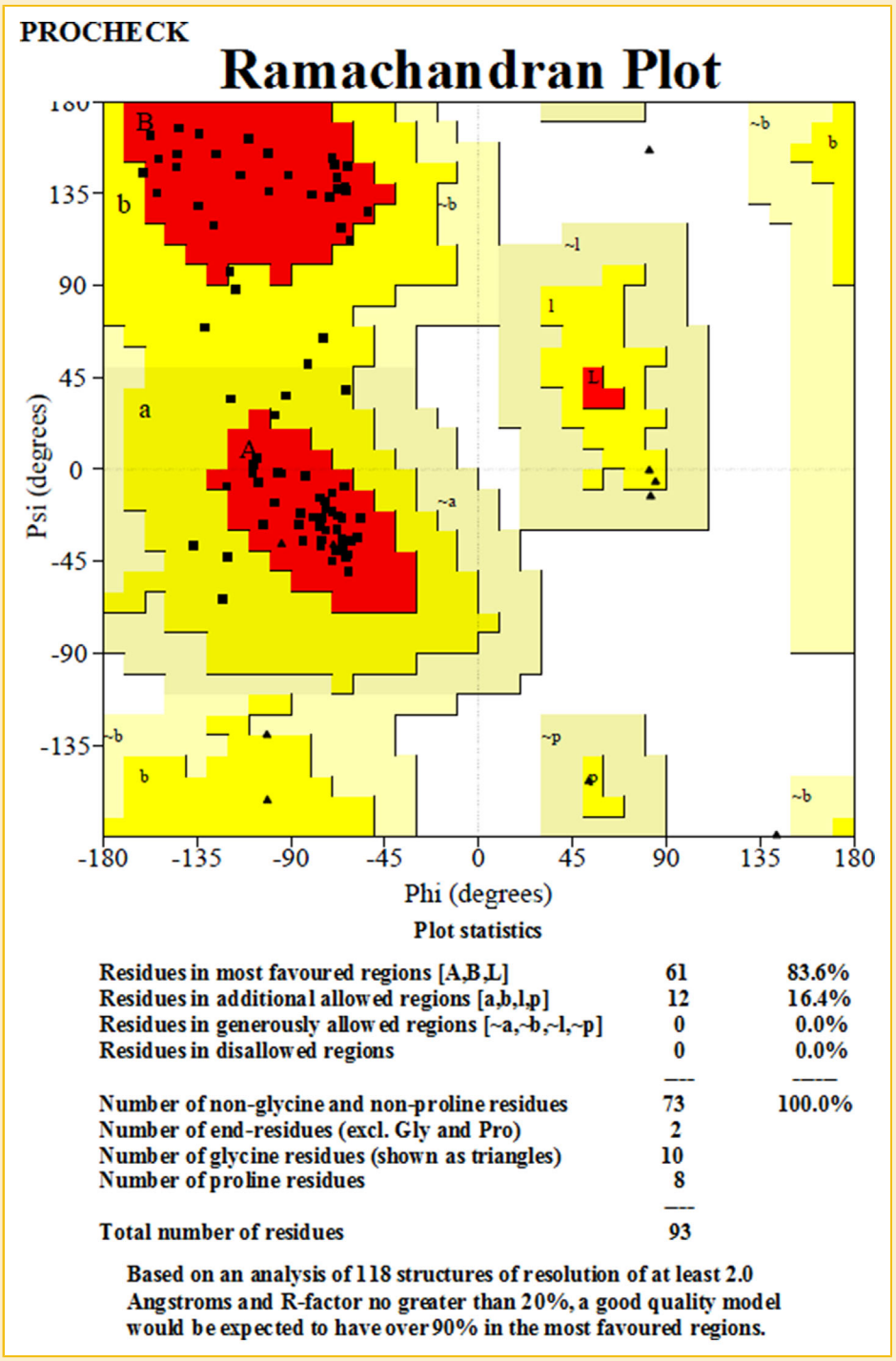


**Fig. 2.** Ramachandran plot of modeled native *rpoB* structure. The most favored regions are represented in red, additional allowed regions in dark yellow, and generously allowed regions in light yellow.

TABLE I. RMP Contacting Residues With Their Interacting Position and the Binding Energy of Both Native and Mutant *rpoB*

| S. no. | Complex types | Contacting residues with position | Binding energy (kcal/mol) |
|---|---|---|---|
| 1 | Native *rpoB* | PHE 399, PHE 400, LEU 405, SER 406 GLN 407, HIS 420 LYS 421, ARG 423 MET 409, LEU 424 SER 425, PRO 429 | 7.324 |
| 2 | Mutant *rpoB* | PHE 399, PHE 400, GLY 401, LEU 405, SER 406, GLN 407, PHE 408, MET 409, HIS 420, LYS 421, ARG 423, LEU 424, LEU425. | 6.865 |

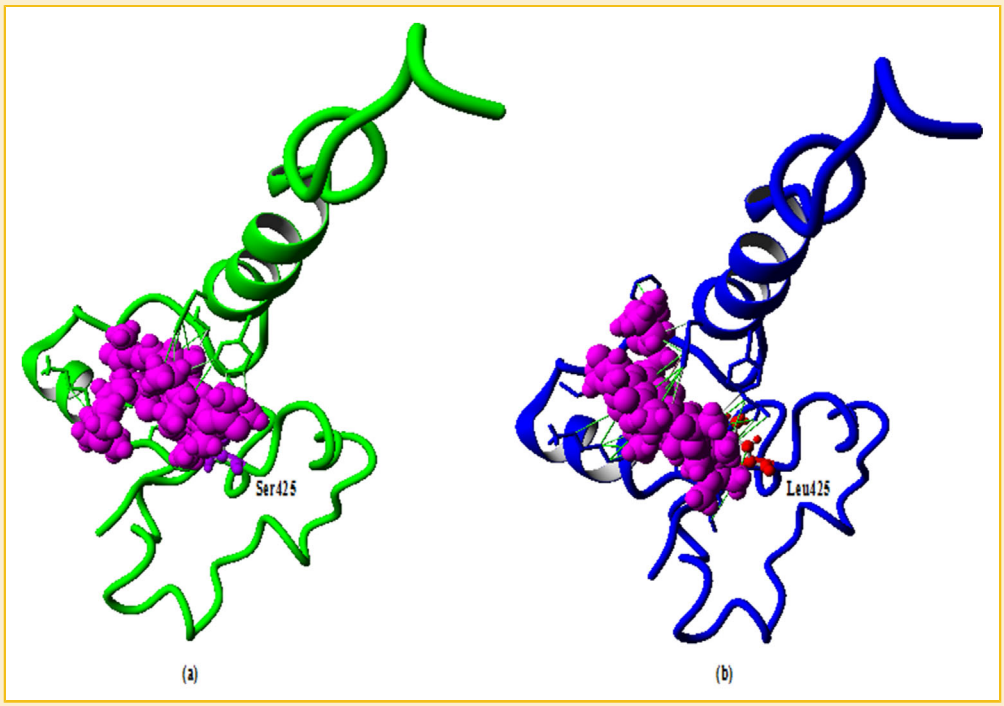


**Fig. 3.** Visualization of docked complexes: molecular docking of RMP with native *rpoB* (A) and mutant *rpoB* (B).

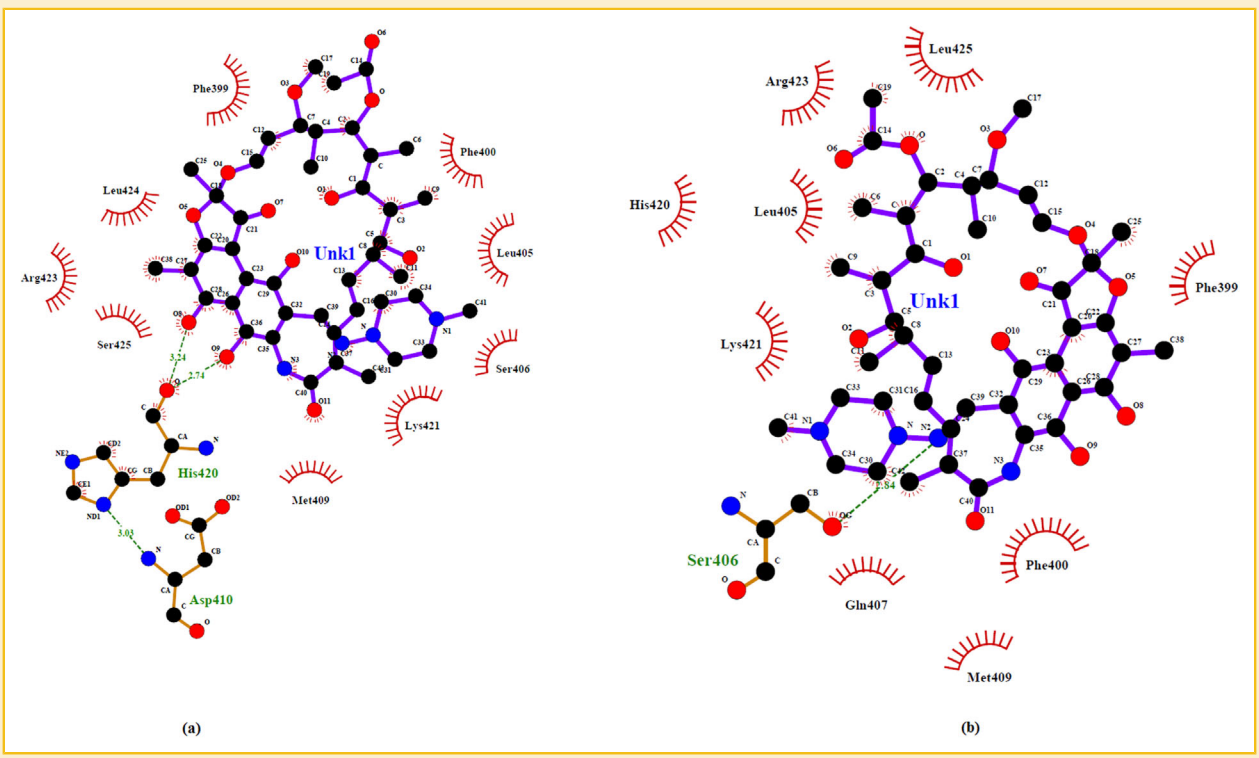


**Fig. 4.** Interaction model of RMP with native *rpoB* (A) and mutant *rpoB* (B). This plot was generated using the LIGPLOT program.

understanding of the complex stability. The lower RMSD value is corresponds to the higher stability of the complex structure and vice versa. The result was shown in Figure 5a. It is clear that both native and the mutant *rpoB*–RMP complex structures showed deviation from their starting structure and reaches stable conformations after 12,500 ps. For instance, RMSD value is in the range of ~0.5 nm was observed in the first 500 ps for both native and mutant complex structures. After 500 ps, native complex showed maximum deviation than the mutant type and attained the RMSD value of ~1.1 nm whereas mutant structure deviated less and maintained the RMSD of ~0.5 nm till 2,000 ps. Both the native and mutant structures showed higher fluctuation between 2,000–7,500ps and attained the RMSD value of ~1.2 nm. However, RMSD value of mutant structure fluctuates even after 7,500 ps and attained 1.4 nm at the end of the simulation time. On the other hand, native complex able to maintain RMSD value of 1.2 nm till the end of simulation period. The lesser RMSD value of native complex structure clearly indicates the formation of stable complex than mutant type structure. We have also examined the flexibility of amino acid residues in the complex structures by means of RMSF analysis. This result is shown in Figure 5b. It is evident from the figure that flexibility of residues significantly higher in the mutant *rpoB*–RMP complex than native *rpoB*–RMP complex. The lesser flexibility of residues in native complex structure is clearly depicts the involvement of those residues in the intermolecular contacts with the partner molecule. It is worth stressing that result of RMSF analysis correlates well with intermolecular contact details obtained in our analysis. It is likely that substitution of the hydrophilic side-chain serine with the hydrophobic side-chain leucine caused disruption of intermolecular contacts in the mutant type and thus decrease the probability of *rpoB*–RMP complex reaching its stable and active conformations. Furthermore, we have also examined the SASA of both native and mutant complexes. The result was shown in Figure 5c. SASA reports for bimolecular surface area that is assessable to solvent molecules.

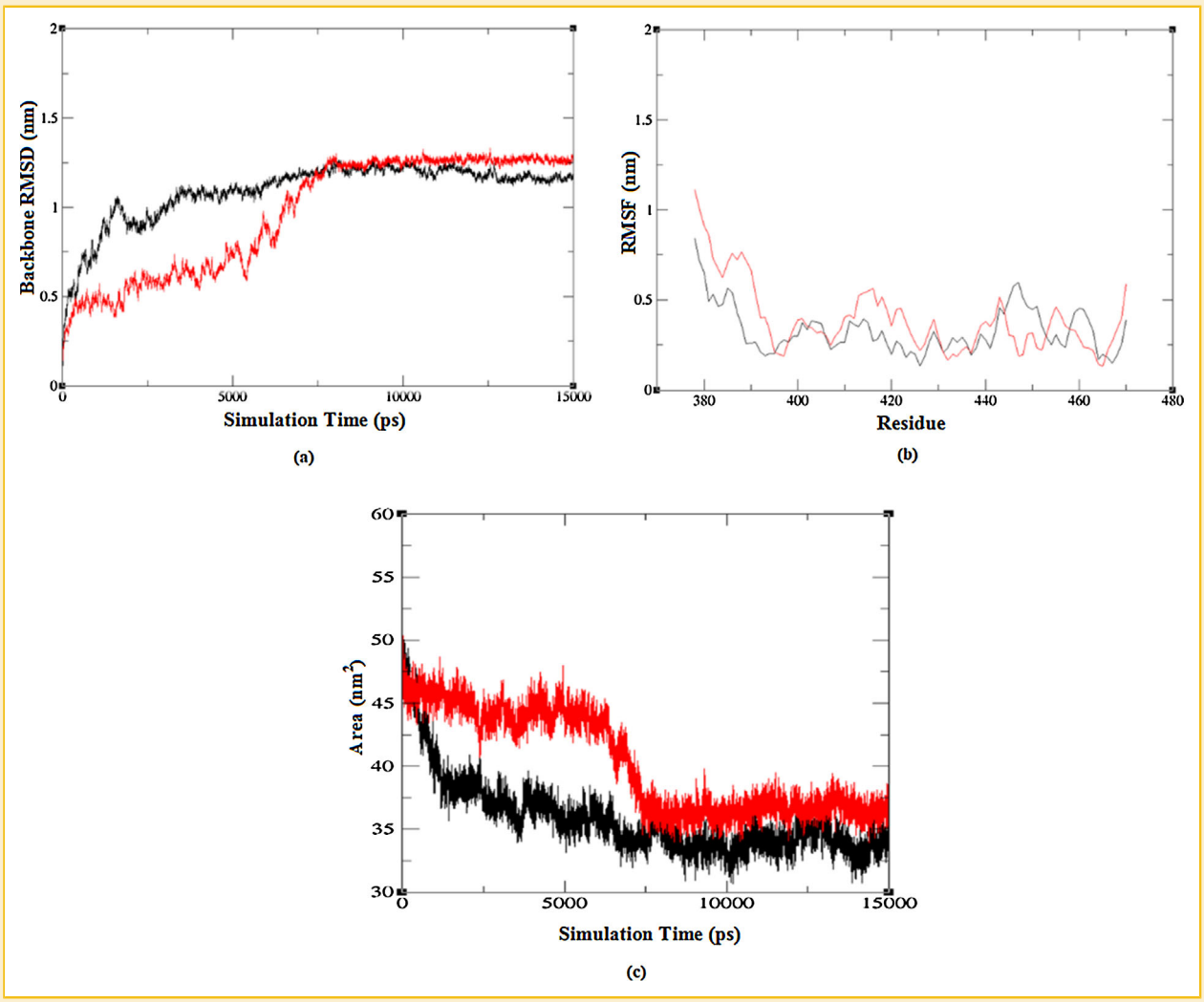


Fig. 5. RMSD (A), RMSF (B), and SASA (C) of native (black) and mutant (red) *rpoB* complexes versus time at 300 K during molecular dynamics simulation.

From Figure 5c, it is also clear that SASA of the mutant structure drastically increased up to 7,500 ps as compared to native structure, indicating that after mutation the overall structure became more unfolded during the simulation. After 7,500 ps, the mutant complex showed greater variation than native complex and reached ~37.5 $nm^2$, whereas native complex reached ~35 $nm^2$ during the simulation. It is believed that the higher value of solvent accessibility of mutant *rpoB* might alter the positions and orientations of side chain residues leading to a distortion of the structural stability and brings improper binding with RMP.

In conclusion, it is certain about the competence of the presently used MDT for leprosy control, as confirmed by the strong decline in disease prevalence ever since its execution, but resistance to one or more antibiotics have been remarked in many areas. Even so, the disease cases have grown recently and there has been a scant of thorough studies concerning relapse occurrences in recent decades. Hence, new drugs are certainly necessary for treating drug-resistant leprosy and novel outlooks are desired to categorize new lead compounds that can pierce the pipeline of lead optimization and therapeutic testing. In this study, we have used the computational approach to investigate the molecular and structural properties of the RMP binding to both native and mutant *rpoB*. The difference in binding energies observed in the docking study evidently signifies that RMP is less effective in the treatment of patients with S425L variant. Most importantly, the interaction maintained by the amino acid residues viz., Phe at position 399, Phe at 400, Leu at 405, Ser at 406, Gln at 407, Met at 409, His at 420, Lys at 421, Arg at 423, Leu at 424, Ser at 425, and Pro at 429 is certainly necessary for the better binding of RMP to the target protein *rpoB*. Also, the results of RMSD, RMSF, and SASA data observed from the molecular dynamics simulation studies certainly indicate the stable binding RMP with native than mutant *rpoB*. Moreover, upon S425L mutation, several features viz., the difference in flexibility of protein back bone, the distinct fluctuations in the mobility of contacting residues, and the alterations in SASA, resulted in considerable changes in the structure, conformation, and function of the mutant *rpoB*. We believe that these computational attempts will help to gain vision into the molecular mechanism of RMP resistance due to S425L mutation. The positive outcome of the computational approach analyzed above foretell the future chances of discovering new therapeutics which could produce considerable cutbacks in therapeutics development time.

## ACKNOWLEDGMENTS

The authors gratefully acknowledge ICMR for funding the research project [no. 5/8/3/5/TF.Lep/2012-ECD-I] and the management of VIT for providing the facilities to carry out this work.

## REFERENCES

Darden T, Perera L, Li. Pedersen. 1999. New tricks for modelers from the crystallography toolkit: the particle mesh Ewald algorithm and its use in nucleic acid simulations. Structure 55–60.

Guex N, Peitsch MC. 1997. SWISS-MODEL and the Swiss-Pdb viewer: An environment for comparative protein modeling. Electrophoresis 18:2714–2723.

Halgren TA. 1996. Merck molecular force field I Basis, form, scope, parameterization and performance of MMFF94. J Comput Chem 17:490–519.

Honore N, Core ST. 1993. Molecular basis of rifampicin resistance in *Mycobacterium leprae*. Antimicrob Agents Chemother 37:414–418.

Jakubík J, Randáková A, Doležal V. 2013. On homology modeling of the M2 muscarinic acetylcholine receptor subtype. J Comput Aided Mol Des. 27:525–538.

Jacobson RR, Hastings RC. 1976. Rifampicin resistant leprosy. Lancet 1304–1305.

Jamet P, Marchoux Chemotherapy Study Group. 1995. Relapse after long-term foolow up of multibacillary patients treated by the WHO multidrug regimen. Int J Lepr other Mycobact Dis 63:195–201.

Ji B. 1987. Drug susceptibility testing of *Mycobacterium leprae*. Int J Lepr 53:830–835.

Ji B. 2002. Rifampicin resistant leprosy: A review and a research proposal of a pilot study. Lepr Rev 73:2–8.

Ji B, Perani EG, Petinom C, Grosset JH. 1996. Bactericidal activities of combinations of new drugs against *Mycobacterium leprae* in nude mice. Antimicrob Agents Chemother 40:393–399.

Ji B, Sow S, Perani E. 1998. Bactericidal activities of a single-dose combination of ofloxacin plus minocycline, with or without rifampicin, against *Mycobacterium leprae* in mice and in lepromatous patients. Antimicrob Agents Chemother 42:1115–1120.

Krieger E, Vriend A. 2002. Models@Home: Distributed computing in bio-informatics using a screensaver based approach. Bioinformatics 18: 315–318.

Krieger E, Darden T, Nabuurs SB, Finkelstein A, Vriend G. 2004. Making optimal use of empirical energy functions: Force-field parameterization in crystal space. Proteins 57:678–683.

Laskowaski RA, Mcarther MW, Moss DS, Thornton JM. 1993. PROCHECK: A program to check the stereochemical quality of protein structure. J Appl Crystal 26:283–291.

Lindahl E, Hess B, van der Spoel D. 2001. GROMACS 3.0: A package for molecular simulation and trajectory analysis. J Mol Model 7:306–317.

Matsuoka M. 2010. Drug resistance in leprosy. Jpn J Infect Dis 63:1–7.

Meagher KL, Carlson HA. 2005. Solvation influences flap collapse in HIV-1 protease. Proteins 58:119–125.

Musser JM. 1995. Antimicrobial agent resistance in mycobacteria: Molecular genetics insights. Clin Microbiol Rev 8:496–514.

O′Boyle NM, Banck M, James CA, Morley C, Vandermeersch T, Hutchison GR. 2011. Open Babel: An open chemical toolbox. J Cheminform 3:33.

Ramachandran GN, Ramakrishnan C, Sasisekharan V. 1963. Stereochemistry of polypeptide chain configurations. J Mol Biol 7:95–99.

Rajasekaran M, Abirami S, Chen C. 2011. Effects of single nucleotide polymorphisms on human N-acetyltransferase 2 structure and dynamics by molecular dynamics simulation. PLoS ONE 6(9):e25801.

Schuttelkopf AW, Van aalten DM. 2004. PRODRG: A tool for high-throughput crystallography of protein-ligand complexes. Acta Crystallog 60:1355–1363.

Schwede T, Kopp J, Guex N, Peitsch MC. 2003. SWISS-MODEL: An automated protein homology-modeling server. Nuc Acids Res 31:3381–3385.

Spoel D, Lindahl E, Hess B, Groenhof G, Mark AE, Berendsen HJ. 2005. GROMACS: Fast, flexible, and free. J Comput Chem 26:1701–1718.

Stewart J. 1990. MOPAC: A semiempirical molecular orbital program. J Comput Aided Mol Des 4:1–103.

Telenti A, Imboden P, Marchesi F. 1993. Detection of rifampicin-resistance mutations in Mycobacterium tuberculosis. Lancet 341:647–650.

Trott O, Olson AJ. 2010. AutoDock Vina: improving the speed and accuracy of docking with a new scoring function, efficient optimization, and multi-threading. J Comput Chem 31:455–461.

Van Gunsteren WF, Billeter SR, Eising AA, Hunenberger PH, Kruger P, Mark AE, Scott WRP, Tironi IG. 1996. Biomolecular simulation: The GROMOS96 manual and user guide. Zurich.

Wallace AC, Laskowski RA, Thornton JM. 1995. LIGPLOT: A program to generate schematic diagrams of protein-ligand interactions. Protein Eng 8:127–134.

WHO Study Group. 1982. Chemotherapy of leprosy for control programmes. WHO Tech Rep Ser 675.

WHO Expert Committee on Leprosy. 1998. Seventh Report WHO. Tech Rep Ser 874.

World Health Organization. 1999. Global leprosy situation. Wkly Epidemiol Rec 74:313–316.

World Health Organization. 2010. Surveillance of drug resistance in leprosy. Wkly Epidemiol Rec 86:389–399.

Williams DL, Gillis TP. 2012. Drug resistant leprosy: Monitoring and current status. Lepr Rev 83:269–281.

Williams D, Waguespack C, Eisenach K. 1994. Characterization of rifampicin resistance in pathogenic mycobacteria. Antimicrob Agents Chemther 38:2380–2386.